

# New Insights into Secondary Metabolite Potential in *Hypericum Perforatum*, UPLC-ESI-MS/MS to Novel Phytochemical Discovery with Bioactivity Assessment

Labza Roumaissa,<sup>[a]</sup> Hamida Saida Cherif,<sup>[a]</sup> Larbi Derbak,<sup>[b]</sup> Petras Rimantas Venskutonis,<sup>[c]</sup> Ibrahim Demirtas,<sup>[d]</sup> Alzahrani Mohammed M,<sup>[e]</sup> Fehmi Boufahja,<sup>[e]</sup> Hamdi Bendif,<sup>[e]</sup> and Stefania Garzoli\*<sup>[f]</sup>

Different anatomical components of *Hypericum perforatum* (*H. perforatum*) have been utilized by humans for generations as a natural remedy with pharmacological attributes. This work aimed to investigate the secondary metabolite potential of *H. perforatum* from Algeria using LC-ESI-MS/MS to determine its phytochemical profile. LC-ESI-MS/MS analysis revealed 22 components, with isoquercitrin being the most abundant bioactive compound at a concentration of 4162 µg/g. The total phenolic and flavonoid contents were also quantified, with TPC equal 171.54 ± 0.79 mg GAE/g and TFC equal 144.26 ± 14.3 mg QE/g. The antioxidant capacity of the extract was evaluated using in vitro assays, showing strong activity with an ABTS IC<sub>50</sub> of

0.173 mg/mL. The antiproliferative potential of the methanolic extract was assessed by the MTT assay on CAPAN-1, DLD-1, and the healthy L929 cell line. The extract exhibited significant antiproliferative effects on CAPAN-1 and DLD-1 cells, with IC<sub>50</sub> values of 0.807 ± 0.06 mg/mL and 0.953 ± 0.03 mg/mL, respectively, whereas no cytotoxicity was observed on L929 cells. Furthermore, SwissADME was used to evaluate the pharmacokinetics and drug-likeness of the main compounds. These findings enhance the understanding of *H. perforatum* and may support its prospective applications in pharmaceutical and cosmetic industries.

## 1. Introduction

According to a literature review, *Hypericum* is a notable genus within the *Hypericaceae* family, consisting of over 500 species<sup>[1]</sup> categorized into 36 sections (Robson, 2006).<sup>[2]</sup> *Hypericum per-*

*foratum* (*H. perforatum*), or St. John's wort, has been utilized in both traditional and contemporary medicine as a treatment for hemorrhoids, diarrhea, and ulcers,<sup>[3,4]</sup> in addition to addressing bruises, burns, swellings, eczema, and psychological disorders including anxiety, neuralgia, and mild to moderate depression.<sup>[5]</sup> It has also been utilized to address fibrositis, sciatica, and menopausal neurosis.<sup>[6]</sup> Moreover, it has been employed to promote vasodilation,<sup>[7]</sup> and prior studies have established its efficacy in addressing chronic stress, Alzheimer's disease, and Parkinson's disease.<sup>[8,9]</sup> The red pigments of *H. perforatum*, hypericin and pseudohypericin, have been documented to possess various bioactivities, including antidepressant, antioxidant, anti-inflammatory, antiviral, antimicrobial, cytotoxic, wound-healing, analgesic, hepatoprotective, and antibacterial effects,<sup>[10,11]</sup> alongside tyrosinase and cholinesterase inhibitory activities<sup>[12,13]</sup> and antiretroviral and anticancer properties.<sup>[14–17]</sup>

Currently, the investigation of antioxidant capacities has become an important topic as the adopted lifestyles are favored to lead to improved health conditions. Consequently, the attention toward botanical products as a source of natural antioxidants has increased. According to some studies, natural antioxidants, including phenolic phytochemicals, might be promising agents for cancer chemoprevention and cancer treatment.<sup>[18]</sup> The antitumor activity of *H. perforatum* has been investigated mainly with photodynamic therapy.<sup>[19,20]</sup> A more recent study also reported the discovery of two new compounds in *H. perforatum*, 2,6,9-trimethyl-8-decene-3,5-dione and 3,7,10-trimethyl-9-undecane-4,6-dione.<sup>[21]</sup> However, the amount of different bioactive compounds in *H. perforatum* may vary

[a] L. Roumaissa, H. S. Cherif  
Biotechnology, Environment and Health Laboratory, Department of Natural and Life Sciences, Faculty of Sciences, Saad Dahlab University, Blida 1, Soumaa road, Blida 09000, Algeria

[b] L. Derbak  
Department of Natural and Life Sciences, Faculty of Sciences, University of M'sila, University Pole, Road Bordj Bou Arreiridj, M'sila 28000, Algeria

[c] P. R. Venskutonis  
Department of Food Science and Technology, Kaunas University of Technology, Radvilėnų pl. 19, Kaunas LT-50254, Lithuania

[d] I. Demirtas  
Department of Pharmaceutical Chemistry, Faculty of Pharmacy, Ondokuz Mayıs University, Samsun 55270, Turkey

[e] A. Mohammed M, F. Boufahja, H. Bendif  
Department of Biology, College of Science, Princess Nourah bint Abdulrahman University, P. O. Box 84428, Riyadh 11671, Saudi Arabia

[f] S. Garzoli  
Department of Chemistry and Technologies of Drug, Sapienza University, Rome 00185, Italy  
E-mail: stefania.garzoli@uniroma1.it

© 2025 The Author(s). ChemistrySelect published by Wiley-VCH GmbH. This is an open access article under the terms of the [Creative Commons Attribution License](#), which permits use, distribution and reproduction in any medium, provided the original work is properly cited.



Figure 1. *H. perforatum* site at harvesting time.

depending on environmental and ecological factors related to the habitat of the plant.<sup>[22]</sup> In Algeria, the practice of herbal medicine has always existed thanks to the biodiversity of the flora particularly rich in these plants.<sup>[23,24]</sup> There are numerous studies on *H. perforatum* however, to the best of our knowledge, the present work is the first to investigate the phytochemical profiles and biological activities of Algerian *H. perforatum*. High-resolution liquid chromatography-ESI-MS-MS (UPLC-ESI-MS) and in silico ADME assessment were applied for chemical characterization and to determine which group of biomolecules were the most potent. In addition, the antioxidant properties were examined in vitro by applying seven assays, namely total antioxidant activity (TAC), radical scavenging activity (DPPH), 2,2'-azino-bis (3-ethylbenzothiazoline 6-sulfonic acid) (ABTS),  $\beta$ -carotene bleaching assay ( $\beta$ -carotene), ferric reducing antioxidant power (FRAP), cupric ion reducing antioxidant capacity (CUPRAC), and oxygen radical absorbance capacity (ORAC). Furthermore, the antitumor potential and antiproliferative activity of the plant extract were estimated against two human cancer cell lines CAPAN-1, DLD-1, and a healthy cell line L929.

## 2. Materials and Methods

### 2.1. Collection of Plant Material

Samples of the flowering aerial components of *H. perforatum* (Figure 1) were gathered from Chr  a, Blida Province, Algeria. The collection location was situated at an elevation of 1217 meters, with geographic coordinates N36  27'50.3'', E002  57'07.7''. Harvesting occurred in mid-July 2022, coinciding with the peak flowering phase. Voucher specimens were submitted to the Laboratory of Biotechnology, Environment, and Health, Faculty of Natural and Life Sciences, University of Blida 1, Algeria. The botanical specimen was identified by Prof. Marie Stella from the University of Blida 1, Algeria, and a voucher specimen (00125BMS) was preserved at the same institution. Subsequent to collecting, the plant material was purified, air-dried, reduced to small fragments, and pulverized into a fine powder (Figure 2).

### 2.2. Preparation of Crude Extract

Aerial parts of *H. perforatum* were dried for 20 days in the shade at the room temperature ( $\sim 25^\circ\text{C}$ ). The aerial parts of the plant have been crushed into small parts with a grinder to get a



Figure 2. The collection of *H. perforatum*.

homogenous drug powder, and stored at  $4^\circ\text{C}$  until use. Fifty g of the dry material were subjected to Soxhlet extraction with 500 mL methanol for 3 h. After evaporation, the crude extract was stored in dark glass bottles at  $4^\circ\text{C}$  until use. Methanol was selected as the extraction solvent because of its well-documented efficiency in recovering a broad spectrum of secondary metabolites from *H. perforatum*, including phenolic acids, flavonoids, and hypericins, thereby ensuring comprehensive analytical profiling.<sup>[25]</sup> While ethanol and aqueous ethanol are more biocompatible, particularly for pharmaceutical applications,<sup>[26]</sup> our choice of methanol was driven by the study's analytical focus and by the need for comparability with prior phytochemical reports.

### 2.3. LC-ESI-MS/MS Analysis

The chemical composition of the extract was determined by LC-ESI-MS/MS using an Agilent 1260 Infinity II LC system, following the method of described by Derbak et al.<sup>[27]</sup> base on the method of Griffith et al.<sup>[28]</sup> with minor modifications. For sample preparation, 50 mg of the methanolic extract were mixed with 1 mL of methanol: *n*-hexane (1:1, v/v), vortexed for 2 min at  $4^\circ\text{C}$ , and centrifuged at 9000 rpm for 10 min at  $4^\circ\text{C}$ . The methanolic phase was collected, diluted (1:9) with distilled water, and filtered through a  $0.45\ \mu\text{m}$  polypropylene syringe filter. An injection volume of  $5.12\ \mu\text{L}$  was used, with the column oven maintained at  $25^\circ\text{C}$ , and a total run time of 30 min. Chromatographic separation was carried out on a reversed-phase Agilent Poroshell 120 EC-C18 column ( $100 \times 3.0\ \text{mm}$ ,  $2.7\ \mu\text{m}$ ). Detection was performed with an Agilent 6460 Triple Quadrupole Mass Spectrometer equipped with an electrospray ionization (ESI) source, operating in both positive and negative ionization modes. Compound identification and quantification were achieved using multiple reaction monitoring (MRM). The mobile phase consisted of eluent A (water with 5 mM ammonium formate, 75%) and eluent B (acetonitrile with 0.1% formic acid, 25%), under isocratic conditions, at a flow rate of  $0.5\ \text{mL/min}$ . Ioniza-

tion parameters were set as follows: gas temperature 350 °C, nebulizing gas flow 11 mL/min, drying gas flow 15 mL/min (nitrogen), and capillary voltage 4000 V.<sup>[29]</sup> The limit of detection (LOD), limit of quantification (LOQ), and linearity range were determined according to Yilmaz et al.<sup>[30]</sup>

## 2.4. Total Phenolic (TPC) and Total Flavonoid Content (TFC)

The TPC in the methanolic extract was determined using the Folin–Ciocalteu reagent according to the protocol described by Singleton et al.<sup>[31]</sup> Gallic acid (GA) was the reference standard. The results were expressed in gallic acid equivalents in 1 mL of extract (mg GAE/mL). The TFC was determined by the aluminum trichloride (AlCl<sub>3</sub>) method and expressed in quercetin equivalents (mg QE/mL).

## 2.5. Biological Activities

### 2.5.1. Antioxidant Capacities

**Total antioxidant activity (TAC):** TAC of methanolic extract was performed according to the method of Prieto et al.<sup>[32]</sup> Aliquot of 0.2 mL of extract solution (1 mg/mL) was mixed with 0.1 mL distilled water, in addition to 3.0 mL reagent mixture (0.6 M sulfuric acid, 28 mM sodium phosphate, and 4.0 mM ammonium molybdate). Subsequently, the reaction mixture was incubated at 95 °C for 90 min in a water bath and after cooling the reagent mixture at room temperature, the absorbance was measured at 695 nm against a blank. The results were expressed as equivalents of ascorbic acid (AAE mg/g of extract).

**DPPH radical scavenging activity:** The in vitro antioxidant activity was performed by using the spectrophotometry method described by,<sup>[33]</sup> where 50 µL of the methanolic extract at different concentrations are mixed with 1950 µL of DPPH solution. Then, the reaction mixtures were incubated in darkness for 30 min at room temperature. The absorbance was calculated at 517 nm. Ascorbic acid,  $\alpha$ -tocopherol and BHT were considered as a standard antioxidant for the comparison. The value of IC<sub>50</sub> was defined as the quantity of an antioxidant necessary to trap 50% of free radicals.

**ABTS<sup>•+</sup> scavenging assay:** The ABTS<sup>•+</sup> scavenging was determined according to the method of Re et al.<sup>[34]</sup> with slight modification. The ABTS<sup>•+</sup> is generated by mixing 38.4 mg ABTS in 10 mL distilled water with 6.6 mg of potassium persulfate. The mixture was then stored in the dark at room temperature for 16 h. The ABTS<sup>•+</sup> solution was diluted with methanol to obtain an absorbance of 0.700 ± 0.02 at 734 nm. Then, 900 µL of ABTS<sup>•+</sup> solution was added to 100 µL of sample solution in methanol at various concentrations. After 6 min, the percentage inhibition at 734 nm was calculated for each concentration against a blank absorbance (methanol).

**$\beta$ -Carotene bleaching assay:** In this assay, the antioxidant capacity was determined by measuring the inhibition of oxidative degradation of  $\beta$ -carotene (discoloration) by the oxidation products of linoleic acid in the extract following the process of Kartal et al.<sup>[35]</sup> First, 0.5 mg of  $\beta$ -carotene were dissolved in 1 mL of chloroform added to the flask with 25 µL of linoleic acid and 200 mg of Tween 40 emulsifier. After evaporation of the chloroform in the rotary evaporator at 40 °C for 10 min, 100 mL of distilled water saturated with oxygen was added with vigorous stirring. From this new emulsion solution 2.5 mL were transferred into different test tubes containing 350 µL of samples prepared at 2.5 mg/mL in methanol. Subsequent to the incubation of the emulsion system for 48 h in the dark at room temperature, the absorbance was read at 490 nm, using a UV spectrophotometer at various time intervals of incubation (0, 2, 24, and 48 h). BHT and  $\alpha$ -tocopherol were used as antioxidant standards for activity comparison.

Bleaching inhibition (%) = 100 ( $\beta$ -carotene content after 24 h of assay/initial  $\beta$ -carotene content)

**Ferric reducing antioxidant power (FRAP):** The assay is based on the reduction of Fe (III) to Fe (II) and was performed using 2.5–0.156 mg/mL of extract diluted in 1 mL of methanol and mixed with 2.5 mL of phosphate buffer (0.2 M, pH 6.6) and 2.5 mL of 1% potassium ferricyanide [K<sub>3</sub>Fe (CN)<sub>6</sub>].<sup>[36]</sup> The mixed solutions were set in the incubator at 50 °C for 20 min. Afterward, 2.5 mL of trichloroacetic acid (10%) were added to each mixture and shaken vigorously. The obtained solution was mixed with 2.5 mL of distilled water and FeCl<sub>3</sub> (0.5 mL, 0.1%), the resulted mixture was incubated for 30 min and the absorbance was measured at 700 nm. The results were expressed in Trolox equivalents (mg TE/mL).

**Cupric ion reducing antioxidant capacity (CUPRAC):** The method of Apak et al.<sup>[37]</sup> was used for CUPRAC. Briefly, aqueous solutions of CuCl<sub>2</sub> (1 mM), ammonium acetate buffer (1 mM at pH 7) and alcoholic solution of neocuproine (Nc) (7.5 mM) were mixed and the absorbance of the corresponding complexes was read after 30 min at 450 nm against a blank reagent.

**Oxygen radical absorbance capacity (ORAC):** The method reported by Prior et al.<sup>[38]</sup> was applied. At first, a phosphate buffer saline solution (75 mmol/L; pH 7.4) and a stock solution of fluorescein were prepared. 25 µL of the diluted methanolic extract (MeOH for blank, or standard trolox for calibration) were pipetted into the 96-well black opaque microplate with transparent flat bottom and mixed with 150 µL of 14 µmol/L fluorescein solution at 37 °C. The reaction mixture was preincubated for 15 min and then 25 µL of AAPH solution (240 mM) were added by using a multichannel pipette. Hence, the microplate was quickly introduced in a FLUOstar Omega fluorescent reader and automatically agitated prior each reading. The fluorescence was measured in total 120 cycles (every 60 s, excitation wavelength: 485 nm, emission wavelength: 520 nm). The results (ORAC value) were exported from the Fluostar Omega Mars software (BMG Labtech GmbH, Offenburg, Germany) and ana-



lyzed in an Excel sheet for extra calculations. The antioxidant capacity as trolox equivalents was determined by calculating the area under the fluorescence decay curve (AUC) relative to the trolox standard calibration. The final ORAC results were calculated in  $\mu\text{M TE/g}$  by using a regression equation between the trolox concentration and the net area under the AUC. All determinations were carried out in triplicates.

### 2.5.2. Determination of in Vitro Antiproliferative Activity

The antiproliferative activity of *H. perforatum* methanolic extract was assessed against CAPAN-1 (pancreatic adenocarcinoma), DLD-1 (colorectal adenocarcinoma), and L929 (mouse fibroblasts, normal control) cell lines following the method described by Ameer et al.,<sup>[39]</sup> with slight changes. All the cell lines were obtained from the laboratory of prof. Dr. Mustafa Türk (Kırıkkale University). Cells were seeded at  $1.0 \times 10^4$  cells per well in 96-well plates (Corning, USA) and incubated for 24 h to allow attachment. Treatments were then applied with various extract concentrations (1.0, 0.75, 0.5, and 0.25 mg/mL) prepared in complete DMEM medium (Sigma-Aldrich, USA). Vehicle control wells contained the same final concentration of DMSO as the treated wells, and extract-only blanks (extract + medium, no cells) were included at each concentration. After 24 h of exposure, the medium was replaced with 100  $\mu\text{L}$  of MTT solution (1 mg/mL in PBS; Sigma-Aldrich, USA), followed by incubation for 2–2.5 h at 37 °C in the dark. Formazan crystals were dissolved with 100  $\mu\text{L}$  of isopropanol (Merck, Germany) per well, and absorbance was measured at 570 nm with a reference at 630 nm using a microplate reader (Thermo Scientific Multiskan GO, USA). No commercial kit was used; all reagents were prepared manually from high-purity analytical grade chemicals (Sigma-Aldrich and Merck). Cell viability (%) was calculated after blank correction using the formula:

$$\text{Cell viability \%} = \frac{A_s}{A_c} \times 100$$

where  $A_s$  and  $A_c$  represent the mean absorbance of treated and vehicle control cells, respectively. Each condition was tested in triplicate and experiments were repeated three independent times.  $\text{IC}_{50}$  and  $\text{IC}_{75}$  values were determined by fitting dose–response curves with a four-parameter logistic (4PL) nonlinear regression model using OriginPro 2021. Results are expressed as mean values with 95% confidence intervals.

### 2.6. Physicochemical and Pharmacokinetic Properties for Computational Methods

The Swiss ADME website allows with free access to evaluate and predict the following physicochemical properties: molecular size, lipophilicity, polarity, insolubility, pharmacokinetics, drug-likeness and medicinal chemistry friendliness of small molecules.<sup>[40]</sup> The programme at <http://www.molsoft.com/mprop/mprop.cgi> detects drug-likenesses and molecular property predictions of biological molecules. pkCSM (<http://structure.bioc.cam.ac.uk/pkCsm>) is an intriguing computational tool that

applies a novel graph-based signature approach to predict pharmacokinetic and toxicity profiles of small molecules. By integrating physicochemical properties, toxicophores, and pharmacophores, pkCSM facilitates the identification of compounds with an optimal balance between potency, pharmacokinetics, and safety, making it a valuable resource in modern drug discovery.<sup>[41]</sup>

### 2.7. Expression of Data and Statistical Analysis

All experiments were performed in triplicate ( $n = 3$ ), and results are expressed as mean  $\pm$  standard deviation (SD). Statistical differences between treatment groups were assessed using one-way ANOVA, with the tested extracts treated as fixed factors. When significance was detected ( $p < 0.05$ ), Tukey's multiple range test was applied for post hoc comparisons.  $\text{IC}_{50}$  values were determined by linear regression analysis in OriginPro 2021. The SwissADME Web tool was used to evaluate the ADMET properties. These procedures were employed to ensure the accuracy, reliability, and reproducibility of the results.

## 3. Results and Discussion

### 3.1. LC-ESI-MS-MS Results

Several studies have elucidated the importance of phenolic compounds in human diet and health, consequently, their extraction processes, chemical characterization, and evaluation of their biological activities have captured immense attention from researchers.<sup>[42]</sup> Reportedly, there are three types of secretory structures including secretory canals, translucent glands, and black nodules, which are sites of collection and synthesis of different secondary metabolites.<sup>[43,44]</sup> The constituents usually differ quantitatively among plants due to genetic variation, climate, habitat, growing conditions, harvesting time, light exposure, and sample extraction techniques.<sup>[45,46]</sup> In the present study, the LC-ESI-MS/MS technique was applied to better understand the biochemical diversity of secondary metabolites, also determining the quantitative profile.<sup>[47]</sup> The chromatogram obtained from the analysis of the methanolic extract of *H. perforatum* is reported in Figure 3.

The LC-ESI-MS/MS fingerprint obtained for the Algerian *H. perforatum* population revealed a coherent chemotype that differs quantitatively and qualitatively from many European reports. In total, 22 compounds were identified and quantified from *H. perforatum* extract in this study (Table 1). Isoquercitrin (4162  $\mu\text{g/g}$ ), quercetin (874  $\mu\text{g/g}$ ), and hyperoside (636  $\mu\text{g/g}$ ) were the major flavonoids, whereas chlorogenic acid (100  $\mu\text{g/g}$ ) and rutin (21.2  $\mu\text{g/g}$ ) were relatively minor. These values are markedly different to these reported for other European populations. For example, Piatti et al.<sup>[48]</sup> quantified hyperoside (18727  $\mu\text{g/g}$ ), isoquercitrin (11895  $\mu\text{g/g}$ ), rutin (1530  $\mu\text{g/g}$ ), and chlorogenic acid (3550  $\mu\text{g/g}$ ) in Polish plants, whereas Orhan et al.<sup>[49]</sup> reported chlorogenic acid (374  $\mu\text{g/g}$ ), hyperoside (805  $\mu\text{g/g}$ ), rutin (1124  $\mu\text{g/g}$ ), and quercetin (39  $\mu\text{g/g}$ ) in Turkish popula-

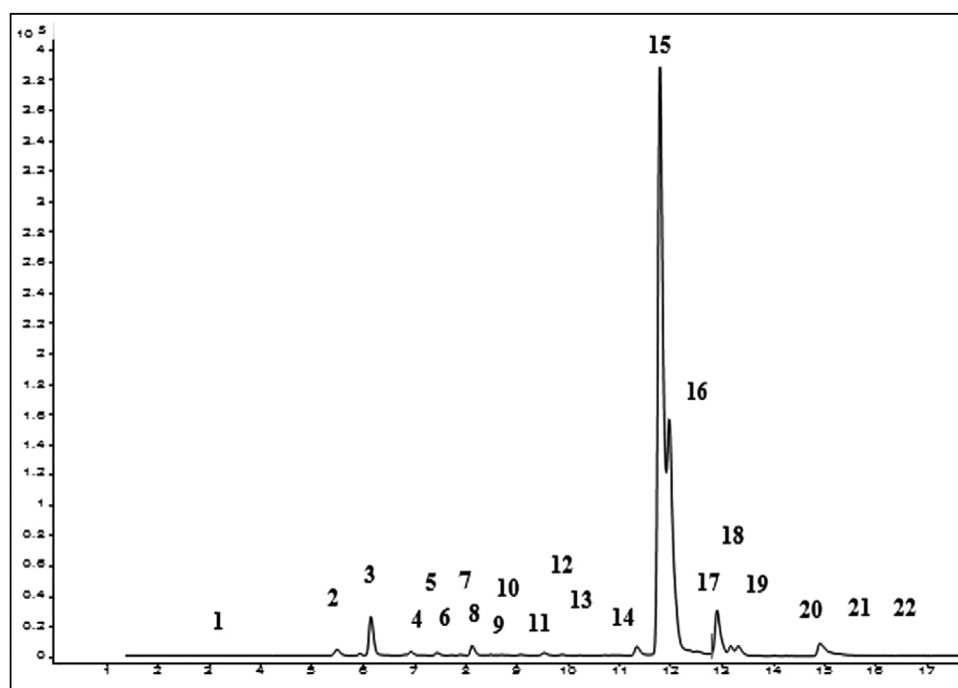


**Figure 3.** Chemical composition of *H. perforatum* methanolic extract. 1. Gallic acid; 2. protocatechuic acid; 3. epigallocatechin; 4. catechin; 5. chlorogenic acid; 6. hydroxybenzaldehyde; 7. vanillic acid; 8. caffeic acid; 9. syringic acid; 10. caffeine; 11. *o*-coumaric acid; 12. polydatin; 13. trans-ferulic acid; 14. hesperidin; 15. isoquercitrin; 16. rutin; 17. quercetin 3-xyloside; 18. kaempferol-3-glucoside; 19. fisetin; 20. quercetin; 21. naringenin; 22. kaempferol.

tions. Compared with these benchmarks, the Algerian population exhibits a consistent reduction in chlorogenic acid, rutin, and hyperoside, while maintaining comparable isoquercitrin and quercetin levels. Such shifts in compound dominance represent a chemotaxonomic signal. Previous Balkan surveys<sup>[50,51]</sup> detected rutin and hyperoside as abundant markers, whereas in Algerian population these compounds are present at much lower levels. This imbalance supports the interpretation that the Algerian population constitutes a low phenolic chemotype distinct from the European type. The observed profile is likely shaped by ecological pressures typical of the Mediterranean environment such as aridity, high solar irradiation, and edaphic factors, which are known to modulate phenolic biosynthesis.<sup>[52]</sup>

### 3.2. Total Phenolic and Flavonoid Contents

Phenolic compounds are considered essential contributors to the antioxidant capacity of plants.<sup>[53]</sup> Therefore, the TPC and TFC of the methanolic extract were measured, and the results are summarized in Table 2. The TPC was  $171.54 \pm 0.79$  mg GAE/g, whereas the TFC was  $144.26 \pm 14.3$  mg QE/g. In terms of TPC, our results were consistent with those reported by Gengiz et al. (2020), who found a TPC value of  $181.02 \pm 1.47$  mg GAE/g in Turkish *H. perforatum* extracts, and were higher than those reported by Ezgi et al.,<sup>[54]</sup> who measured  $90.40 \pm 1.28$   $\mu$ g PEs/mg extract. Marah et al.<sup>[55]</sup> reported TPC values ranging from  $142.96 \pm 0.76$  to  $155.87 \pm 0.83$  mg GAE/g in aqueous extracts. In contrast, Makarova et al.<sup>[25]</sup> reported higher TPC values, ranging from 317.6 to 402.2 mg GAE/g for ethanol–water extracts and from 199.6 to 298.2 mg GAE/g for ethanol extracts, with

Makarova et al.<sup>[25]</sup> specifically reporting 371 mg GAE/g. Previous studies also reported TPC values of 142 mg GAE/g and 222 mg GAE/g for ethanol–water extracts of *H. perforatum* from Romania Stef et al.<sup>[56]</sup> and Bulgaria Katsarova et al. (2017), respectively. In terms of TFC, Gengiz et al. (2020), Ersoy et al.,<sup>[57]</sup> and Özkan et al.<sup>[58]</sup> reported TFC values of  $66.73 \pm 0.22$  mg RE/g,  $62.49 \pm 0.77$   $\mu$ g QE/mg extract, and  $0.55 \pm 0.03$  mg QE, respectively, using methanol maceration-shake extraction. Other studies reported TFC values ranging from 100.4 to 167.8 mg CAE/g for ethanol extracts and from 138.4 to 175.3 mg CAE/g for ethanol–water extracts, with Makarova et al.<sup>[25]</sup> reporting 160 mg CAE/g. These fluctuations from one extract to another could be related to many factors such as extraction method, processing conditions and storage, which are crucial factors in determining the polyphenol content.<sup>[59]</sup>

### 3.3. Antioxidant Activity

In order to evaluate the antioxidant potential of phytocomplexes, it is essential to measure the antioxidant capacity of their extracts using rapid in vitro assays, and it is very significant to use more than one antioxidant assay.<sup>[60]</sup> In this study, seven complementary assays (DPPH<sup>•</sup>, ABTS<sup>•+</sup>, TAC,  $\beta$ -carotene, FRAP, CUPRAC and L-ORAC) were performed to estimate the in vitro antioxidant properties of the methanolic extract of *H. perforatum*, the results are presented in Table 3.

Needless to say, *H. perforatum* has been also the topic of a vast spectrum of antioxidant capacity studies by various in vitro and in vivo methods.

**Table 1.** Phenolic compounds identified and quantified by LC-ESI-MS/MS analysis of *H. perforatum* methanolic extract.

No.	Compound	<sup>a)</sup> RT (min)	Concentration (ug/g)	Ion transitions	Ion mode	<sup>b)</sup> R <sup>2</sup>	<sup>c)</sup> LOQ (ug/L)	<sup>d)</sup> LOD (ug/L)	Linearity range (ug/L)
1	Gallic acid	3.2	11.4	169.0–125.0	Negative	0.9986	18.5862	7.1674	31.25–500
2	Protocatechuic acid	5.5	127.6	153.0–109.0	Negative	0.9969	13.173	3.156	15.625–250
3	Epigallocatechin	6.8	1.19	307.0–139.0	Negative	0.9991	265.9	237.5	1250–20000
4	Catechin	7.2	347.2	288.9–245.1	Negative	0.9946	7.5013	1.7055	343.750–5500
5	Chlorogenic acid	7.4	100.2	353.0–191.0	Negative	0.9981	25.902	11.589	31.25–500
6	Hydroxybenzaldehyde	7.7	1.87	121.0–92.0	Negative	0.9993	12.865	4.9742	15.625–250
7	Vanillic acid	7.8	179.6	167.0–151.8	Negative	0.9958	164.421	141.042	1250–20000
8	Caffeic acid	7.9	15.3	178.9–135.1	Negative	0.9994	24.162	6.920	31.25–500
9	Syringic acid	8.4	54.06	197.1–181.8	Negative	0.999	165.327	138.541	1250–20000
10	Caffein	8.5	2.38	195.0–137.9	Positive	0.9986	15.4959	6.8099	18.75–300
11	o-Coumaric acid	9.5	15.92	163.0–119.1	Negative	0.9996	7.9973	4.016	15.625–500
12	Polydatin	9.8	0.633	390.9–228.9	Positive	0.9987	1.8411	1.1471	7.8125–125
13	Trans-ferulic acid	10.2	18.6	193.1–133.9	Negative	0.995	11.5276	6.1184	31.25–1000
14	Hesperidin	12.0	20.5	611.0–302.9	Positive	0.9957	17.675	4.139	31.25–500
15	Isoquercitrin	12.0	4162	464.9–302.8	Positive	0.9982	11.268	9.938	18.75–300
16	Rutin	12.4	21.2	608.9–299.4	Positive	0.998	240.672	59.5597	125–2000
17	Quercetin 3-xyloside	12.4	636	464.8–02.8	Positive	0.999	69.4059	18.7126	125–2000
18	Kaempferol-3-glucoside	13.3	109	448.8–286.9	Positive	0.9997	4.5238	1.161	7.8125–125
19	Fisetin	13.3	1.34	287.0–137.0	Positive	0.9954	44.366	10.896	15.625–250
20	Quercetin	15.0	874	300.7–150.9	Negative	0.9964	16.9127	4.6558	27.5–440
21	Naringenin	15.2	6.45	270.9–119.1	Negative	0.996	0.4575	1.369	31.25–500
22	Kaempferol	16.5	86.27	284.9–116.9	Negative	0.9997	5.4004	1.8683	312.5–10000

<sup>a)</sup> RT: retention time.  
<sup>b)</sup> R<sup>2</sup>: coefficient of determination.  
<sup>c)</sup> LOQ (μg/L): limit of quantification.  
<sup>d)</sup> LOD (μg/L): limit of detection.

**Table 2.** Determination of total phenolic content and flavonoid content in *H. perforatum* methanolic extract.

Sample	<sup>a)</sup> TPC (mg <sup>c)</sup> GAE/mL	<sup>b)</sup> TFC (mg <sup>d)</sup> QER/mL
<i>H. perforatum</i> MeOH Ext	171.54 ± 0.79	144.26 ± 14.3

<sup>a)</sup> TPC: total phenolic content.  
<sup>b)</sup> TFC: total flavonoids content.  
<sup>c)</sup> GAE: gallic acid equivalent.  
<sup>d)</sup> QER: quercetin equivalent.  
MeOH Ext: methanol extract.  
Values were expressed as means ± SD (n = 3).

**TAC:** The total antioxidant capacity of the methanolic extract was evaluated using the phosphomolybdenum technique, which is based on the reduction of molybdenum (IV) to molybdenum (V), followed by the formation of green molybdenum (V) phosphate components with maximum absorption at 695 nm. The total antioxidant capacity of the extract was significant with a value of  $0.311 \pm 0.697$  mg AAE/mg, compared to Sarikurcu Cengiz et al.<sup>[61]</sup> who reported a value of  $0.145 \pm 4.69$  mg AAE/mg.

**DPPH<sup>•</sup>:** In this experiment, the *H. perforatum* extract exhibited a concentration dependent scavenging activity against DPPH<sup>•</sup> radicals, with an IC<sub>50</sub> value of  $0.446 \pm 0.061$  mg/mL.

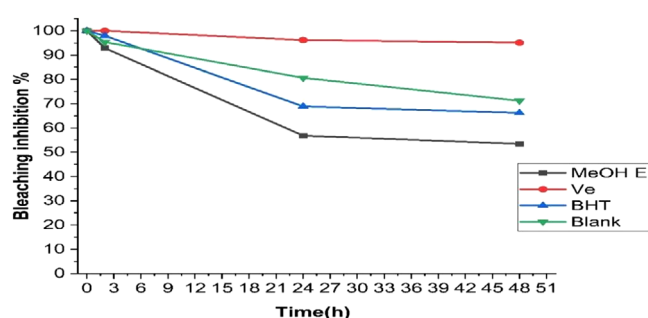
When compared the result to reference antioxidants, the extract reveal lower radical scavenging activity than ascorbic acid ( $0.089 \pm 0.003$  mg/mL), α-tocopherol ( $0.013 \pm 0.002$  mg/mL), BHT ( $0.148 \pm 0.001$  mg/mL), and Trolox ( $0.021 \pm 0.01$  mg/mL) which all had significantly lower IC<sub>50</sub> values, indicating stronger reducing capacities. Our findings are consistent with previous studies where *H. perforatum* extracts displayed lower scavenging potential than pure antioxidant standards. For instance, Ersoy et al.<sup>[57]</sup> and Kakouri et al.<sup>[62]</sup> also noted that *H. perforatum* methanolic extracts required higher concentrations to achieve 50% inhibition compared to synthetic antioxidants.

**Table 3.** In vitro antioxidant activity of *H. perforatum*.

Samples	DPPH IC <sub>50</sub> (mg/mL)	ABTS	TAC (mg AAE/mg)	FRAP (mg TE/mg)	TEAC CUPRAC	TEAC ORAC	$\beta$ -Carotene bleaching (%)
<i>H. perforatum</i> MeOH Ext	0.446 <sup>a</sup> $\pm$ 0.06	0.173 <sup>a</sup> $\pm$ 0.004	0.311 <sup>a</sup> $\pm$ 0.69	2.067 <sup>a</sup> $\pm$ 0.03	0.694 <sup>a</sup> $\pm$ 0.02	1.2 <sup>a</sup> $\pm$ 83.92	56.8 <sup>a</sup> $\pm$ 2.06
Ascorbic acid	0.089 <sup>b</sup> $\pm$ 0.01	0.024 <sup>b</sup> $\pm$ 0.01	0.176 <sup>b</sup> $\pm$ 0.08	2.85 <sup>b</sup> $\pm$ 0.04	2.010 <sup>b</sup> $\pm$ 0.026	4.3 <sup>b</sup> $\pm$ 0.11	NT
$\alpha$ -Tocopherol	0.013 <sup>c</sup> $\pm$ 0.01	0.07 <sup>c</sup> $\pm$ 0.01	NT	1.12 <sup>c</sup> $\pm$ 0.03	1.580 <sup>c</sup> $\pm$ 0.021	2.15 <sup>c</sup> $\pm$ 0.09	96.18 <sup>c</sup> $\pm$ 1.05
BHT	0.148 <sup>c</sup> $\pm$ 0.01	0.073 <sup>c</sup> $\pm$ 0.01	NT	NT	NT	NT	68.88 <sup>d</sup> $\pm$ 1.25
Trolox	0.021 <sup>c</sup> $\pm$ 0.01	0.031 <sup>b</sup> $\pm$ 0.01	0.2 <sup>c</sup> $\pm$ 0.06	–	–	–	NT

BHT: butylated hydroxytoluene; TE: trolox equivalents; AAE: ascorbic acid equivalents; MeOH Ext: methanol extract; NT: not tested. Data are mean  $\pm$  standard error of the mean (SEM),  $n = 3$ .

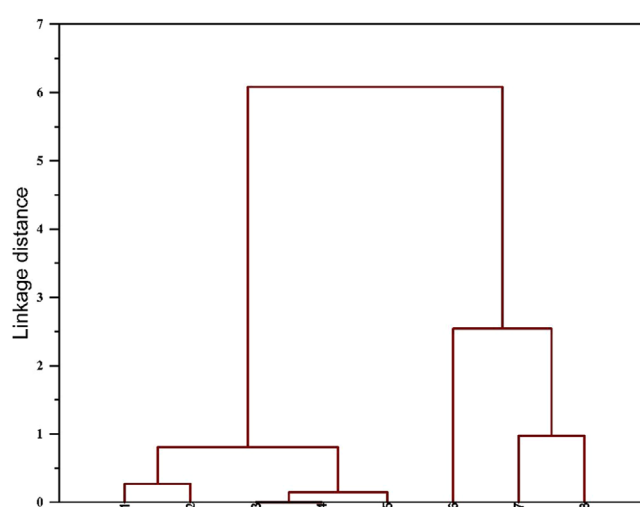
Values in the same column followed by different letters (a–d) are significantly different at  $p < 0.05$  (Tukey's test).

**Figure 4.** Kinetics of  $\beta$ -carotene bleaching at 490 nm in the absence and presence of methanol extract.

**ABTS<sup>+</sup>:** In the ABTS<sup>+</sup> assay, the extract exhibited an IC<sub>50</sub> value of  $0.173 \pm 0.004$  mg/mL, indicating a moderate radical scavenging capacity. This value is significantly higher than the IC<sub>50</sub> announced by Ersoy et al.<sup>[57]</sup> and Kakouri et al.<sup>[62]</sup> for *H. perforatum* methanolic extracts ( $0.009 \pm 0.19$  mg/mL;  $0.006 \pm 0.93$  mg/mL, respectively), suggesting lower antioxidant efficiency in our tested extract. The observed discrepancy may be referred to differences in extraction solvents, geographical origin of the plant material, and phenolic composition, as previously emphasized in interspecies comparisons of *Hypericum*.<sup>[62,63]</sup> Nevertheless, our findings confirm the ability of *H. perforatum* to scavenge ABTS<sup>+</sup>, although with lower potency compared to synthetic antioxidants such as BHT,  $\alpha$ -tocopherol, and ascorbic acid.

**$\beta$ -Carotene bleaching :** According to the Figure 4, after 24 h incubation at 2 mg/mL, *H. perforatum* methanolic extract achieved an inhibition of  $56.8 \pm 2.06\%$ , closely approaching BHT ( $68.88 \pm 1.25\%$ ) and indicating substantial antioxidant capacity in the lipid peroxidation model. This activity aligns with results from a comparative study of water extracts in which *H. perforatum* exhibited a  $\beta$ -carotene bleaching value of  $77.00 \pm 0.32\%$  Sarikurkcü et al. (2020). These data collectively reinforce the extract's meaningful inhibition of lipid oxidation.

**FRAP:** The FRAP assay demonstrated that the methanolic extract of *H. perforatum* revealed a strong ferric-reducing potential, reaching  $2.067 \pm 0.003$  mg TE/mg. This value is substantially higher than those reported in several recent reports. For

**Figure 5.** Cluster analysis revealing the association between total phenolic content and antioxidant capacity assays of *H. perforatum*. (1: TPC, 2: TAC, 3: DPPH, 4: ABTS, 5:  $\beta$ -carotene, 6: FRAP, 7: CUPRAC, and 8: L-ORAC).**Table 4.** Antiproliferative effect of *H. perforatum* on cancer cell lines.

Concentration (mg/mL)	Cell viability % DLD-1	CAPAN-1	L929
1	33.49 <sup>a</sup> $\pm$ 2.03	48.94 <sup>a</sup> $\pm$ 2.14	109.19 <sup>a</sup> $\pm$ 7.63
0.5	177.65 <sup>b</sup> $\pm$ 3.13	71.82 <sup>b</sup> $\pm$ 3.15	254.97 <sup>b</sup> $\pm$ 6.63
0.25	215.44 <sup>c</sup> $\pm$ 5.46	200.56 <sup>c</sup> $\pm$ 4.32	414.23 <sup>c</sup> $\pm$ 9.15
0.125	226.52 <sup>d</sup> $\pm$ 5.14	222.86 <sup>d</sup> $\pm$ 4.87	419.54 <sup>d</sup> $\pm$ 8.69
Control absorbance	0.24	0.24	0.12
IC <sub>50</sub> (mg/mL)	0.96 $\pm$ 0.03	0.81 $\pm$ 0.06	> 1.0
IC <sub>75</sub> (mg/mL)	0.85 $\pm$ 1.04	0.71 $\pm$ 1.11	> 1.0

Data are mean  $\pm$  standard error of the mean (SEM),  $n = 3$ . Values in the same column followed by different letters (a–d) are significantly different at  $p < 0.05$  (Tukey's test).

instance, Piatti et al.<sup>[48]</sup> observed FRAP values ranging between 1.18 and 1.56 mg TE/mg depending on the flowering stage, whereas Błońska-Sikora et al.<sup>[64]</sup> found values between 0.95 and 1.4 mg TE/mg for various *H. perforatum* extracts. Similarly, Doğan

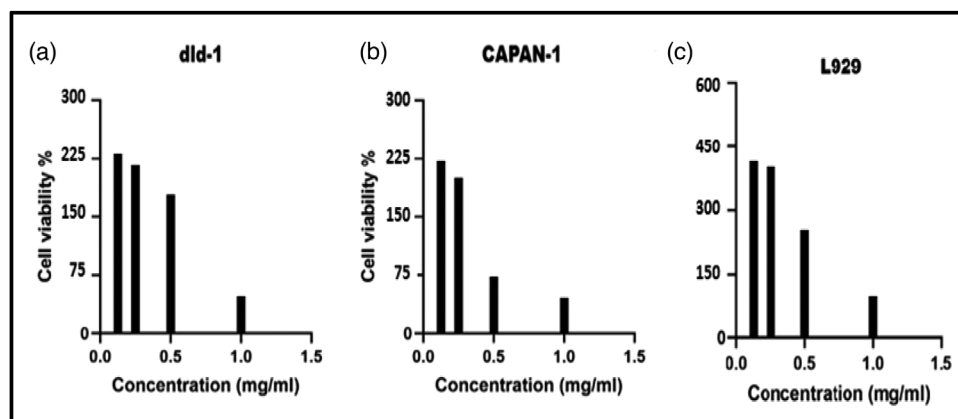


Figure 6. Antiproliferative activity of methanolic extract of *H. perforatum* against DLD-1, CAPAN-1, and L929 cell line.

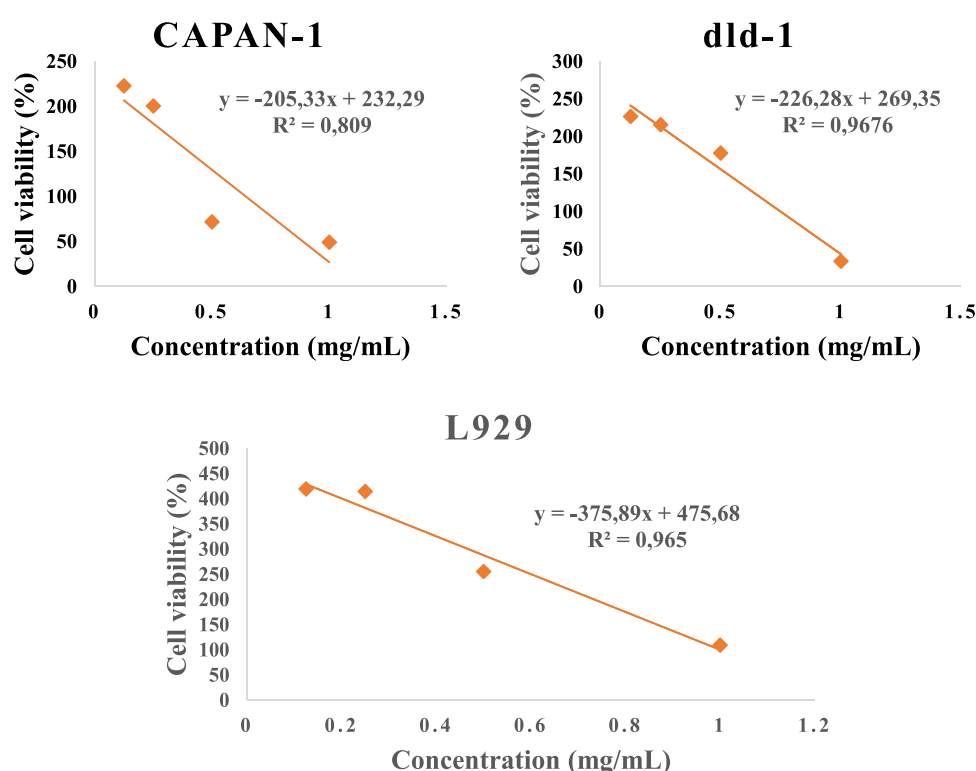


Figure 7. Regression trendline exhibits the correlation between concentration and cell viability (%).

et al.<sup>[65]</sup> reported values around 1200–1350 mg TE/g in aerial parts, and Kurt et al.<sup>[66]</sup> reported approximately 1.65 mg TE/mg when formulating *H. perforatum* into a nanoemulsion hydrogel.

**Cuprac:** In the current study, the methanolic extract of *H. perforatum* exhibited a CUPRAC value of  $0.694 \pm 2.37$  mg TE/mg, highlighting a strong reducing potential. Comparing to previous studies, our value is substantially higher. Piatti et al.<sup>[48]</sup> reported CUPRAC values between 0.143 and 0.386 mg TE/mg depending on the flowering stage, which are clearly lower than our result. Similarly, Sarikurkcu Cengiz et al.<sup>[61]</sup> reported a significant CUPRAC activity of *H. perforatum*, quantified as  $0.268 \pm 5.32$  mg BHAEs/mg extract.

**ORAC:** This test, based on the inhibition of the peroxy radical generator induced by the thermal decomposition of azo-compounds such as AAPH. Our results show an ORAC value of  $1.2 \pm 83.92$  mg TE/mg, which is considerably higher than those reported in previous studies. For instance, Makarova et al.<sup>[25]</sup> detected ORAC values of  $9.701 \mu\text{mol TE/mg}$  in ethanol extracts of air-dried flowers and  $0.775 \mu\text{mol TE/mg}$  in ethanol extracts of lyophilized flower samples, whereas Katsarova et al.<sup>[67]</sup> reported that ethanolic extracts demonstrated a value  $5.95 \pm 328.4 \mu\text{mol TE/mg}$ . The higher ORAC value observed in our extract could be related to the elevated levels of TPC and TFC detected.



Table 5. ADME properties of the <i>H. perforatum</i> identified compounds.																				
Entry	The <i>H. perforatum</i> identified compounds										The <i>H. perforatum</i> identified compounds									
	1	2	3	4	5	6	7	8	9	10	11	12	13	17	18	19	20	21		
Physicochemical properties/lipophilicity																				
Molecular weight	170.12	154.12	306.27	290.27	354.31	228.24	168.15	180.16	198.17	194.19	164.16	390.38	194.18	434.35	448.38	286.24	302.24	272.25		
No. heavy atoms	12	11	22	21	25	17	12	13	14	14	12	28	14	31	32	21	22	20		
TPSA (Å²)	97.99	77.76	130.61	110.38	164.75	46.53	66.76	77.76	75.99	61.82	57.53	139.84	66.76	190.28	190.28	111.13	131.36	86.99		
Consensus Log <i>P</i> <sub>ow</sub>	0.21	0.65	0.42	0.83	−0.39	2.52	1.08	0.93	0.99	0.08	1.4	0.64	1.36	0.10	−0.09	1.55	1.23	1.84		
Drug-likeness/bioavailability/pharmacokinetics																				
Lipinski's rule	Yes	Yes	Yes	Yes	Yes	Yes	Yes	Yes	Yes	Yes	Yes	Yes	Yes	No	No	Yes	Yes	Yes		
BAS	0.56	0.56	0.55	0.55	0.11	0.55	0.85	0.56	0.56	0.55	0.85	0.55	0.85	0.17	0.17	0.55	0.55	0.55		
GI absorption	High	High	High	High	Low	High	High	High	High	High	High	High	High	Low	Low	High	High	High		
BBB permeant	No	No	No	No	No	Yes	No	No	No	No	Yes	No	Yes	No	No	No	No	No		
TPSA: topological polar surface area; Log <i>P</i> : lipophilicity; BAS: bioavailability score; GI: gastrointestinal; BBB: blood–brain barrier. 1. gallic acid; 2. protocatechuic acid; 3. epigallocatechin; 4. catechin; 5. chlorogenic acid; 6. hydroxybenzaldehyde; 7. vanillic acid; 8. caffeic acid; 9. syringic acid; 10. caffein; 11. o-coumaric acid; 12. polydatin; 13. trans-ferulic acid; 14. hesperidin; 15. isoquercitrin; 16. rutin; 17. quercetin 3-xyloside; 18. kaempferol-3-glucoside; 19. fisetin; 20. quercetin; 21. naringenin.																				

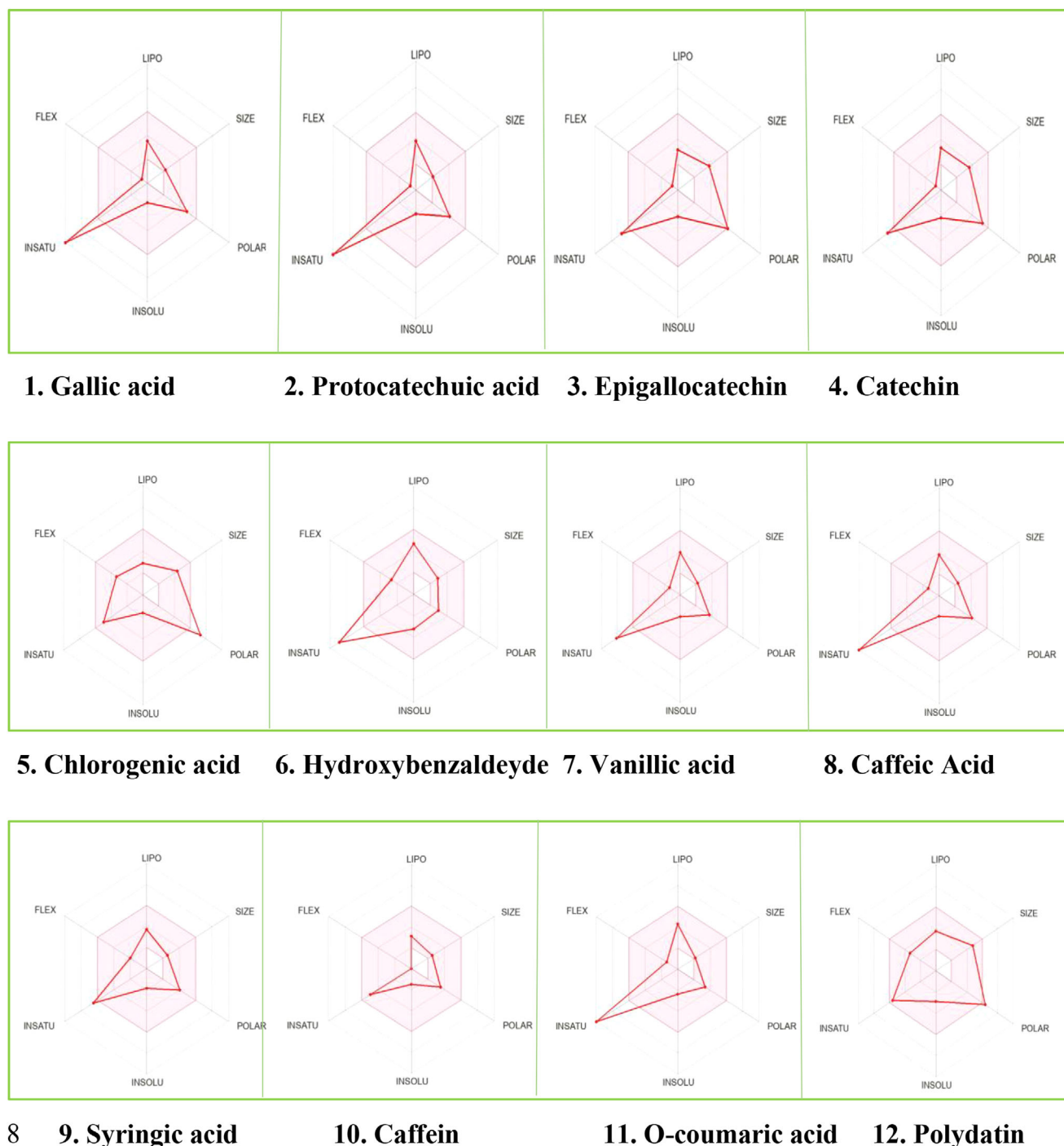


**Figure 8.** Bioavailability hexagons of the major substances identified in *H. perforatum* as assessed by LC-ESI-MS/MS analysis of the methanolic extract. A: lipophilicity; B: molecular size; C: polarity; D: insolubility; E: insaturation; F: flexibility.

### 3.4. HCA Results

Figure 5 illustrates the various clusters and correlations among the antioxidant capacity assays and TPC of *H. perforatum*. Euclidean distance was applied as the distance scale and Ward's method as the linkage rule. The hierarchical cluster analysis separated the antioxidant assays into two principal groups. The first group included DPPH and ABTS, which clustered closely, together with  $\beta$ -carotene bleaching, reflecting their common

radical scavenging mechanism. The second group comprised FRAP, CUPRAC, ORAC, and TPC, demonstrating a strong association between phenolic content and reducing power assays. This clustering pattern indicates that the antioxidant capacity of *H. perforatum* methanolic extract is substantially driven by its phenolic constituents, which mainly act as electron donors and therefore show strong performance in reducing power assays (FRAP, CUPRAC, and ORAC), whereas radical scavenging assays present a distinct clustering behavior.

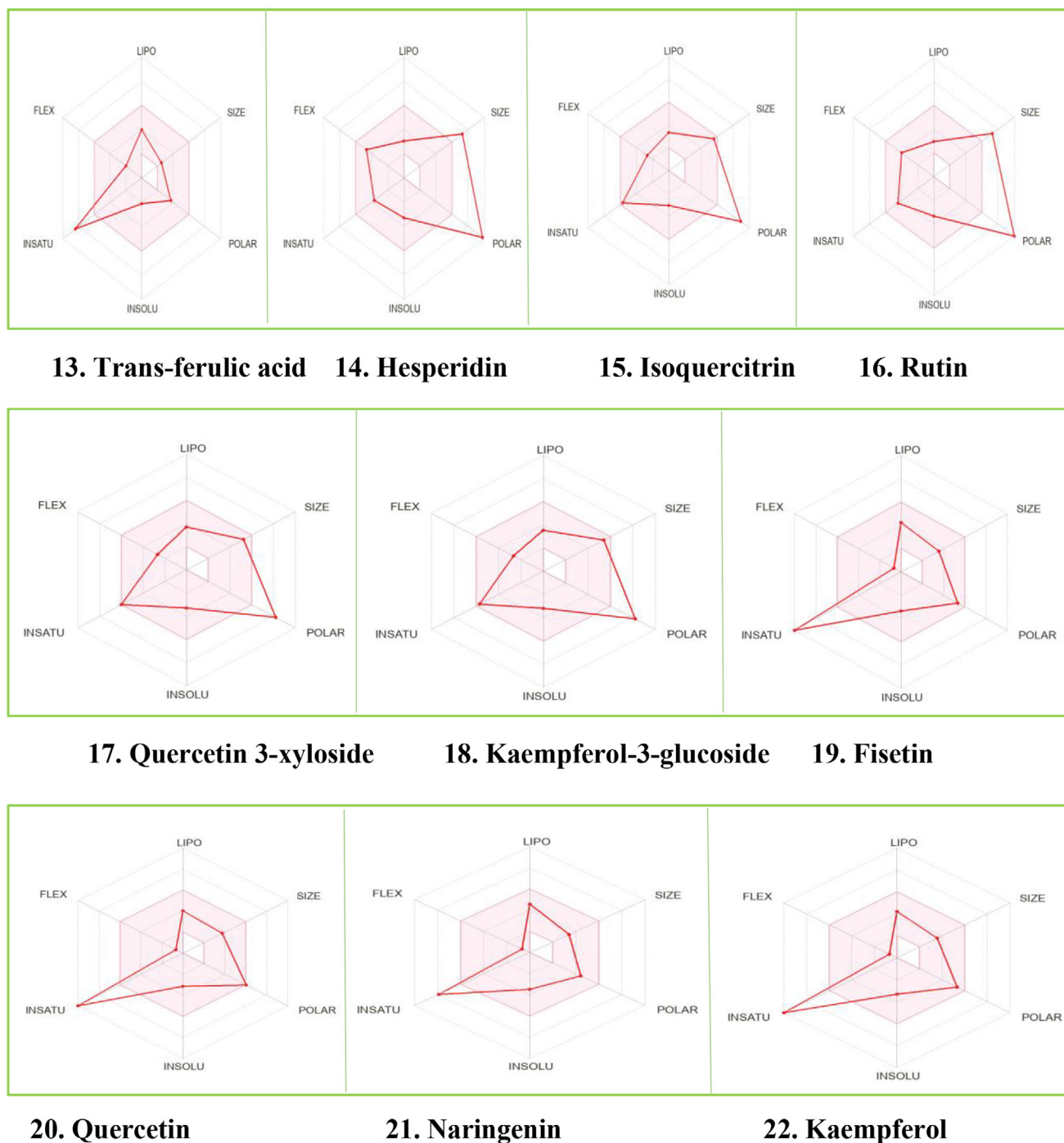


Figure 8. Continued

### 3.5. Antiproliferative Activity

The antiproliferative activity of *H. perforatum* extract on L929 (fibroblast cell line), CAPAN-1 (pancreatic cancer cell line), and DLD-1 (colorectal adenocarcinoma cell line), were carried out using the MTT assay and determined by treating cells with different concentrations of the *H. perforatum* methanolic extract (0.125, 0.25, 0.5, and 1 mg/mL).  $IC_{50}$  and  $IC_{75}$  values were estimated from nonlinear regression curves (4PL model), ensuring accurate dose-response fitting. The results are tabulated in Table 4.

The results of antiproliferative activity outline that treatment of cells with higher concentrations of methanolic extract of *H. perforatum* caused significant damage to the integrity of the cell membrane, in contrast to low concentrations (Figure 6). Various concentrations of *H. perforatum* methanolic extract showed an antiproliferative effect on DLD-1 and CAPAN-1 cell lines with an  $IC_{50}$  value of  $0.953 \pm 0.03$  and  $0.807 \pm 0.06$  mg/mL, respectively, and above 1 mg/mL for the L929 cell line.

Thus, they demonstrated an  $IC_{75}$  value similar to the  $IC_{50}$  values, which confirmed by the evaluation of a simple linear

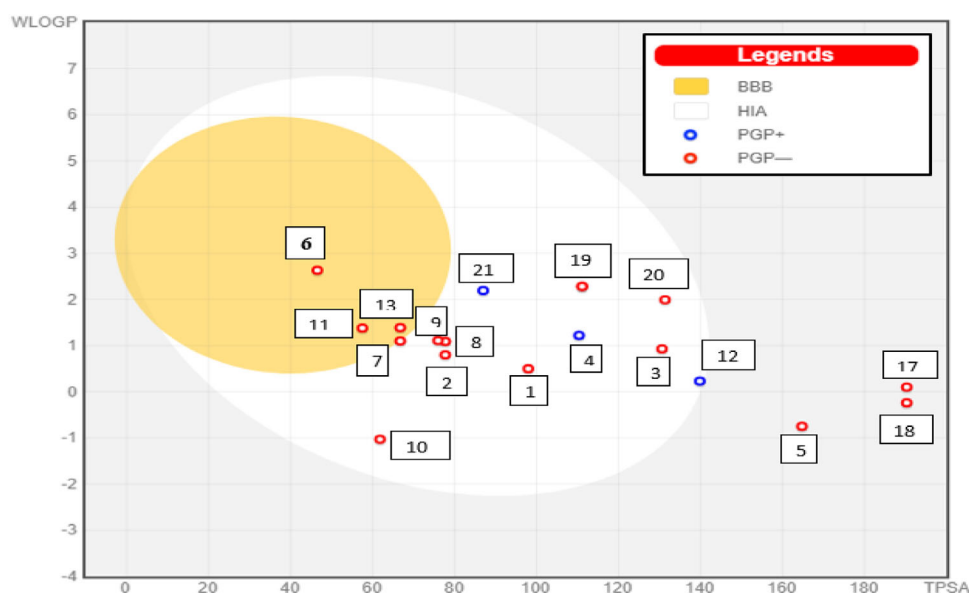


**Figure 9.** Boiled-egg model of *H. perforatum* identified compounds as assessed by LC-ESI-MS/MS analysis of the methanolic extract. 1. Gallic acid; 2. protocatechuic acid; 3. epigallocatechin; 4. catechin; 5. chlorogenic acid; 6. hydroxybenzaldehyde; 7. vanillic acid; 8. caffeic acid; 9. syringic acid; 10. caffeine; 11. *o*-coumaric acid; 12. polydatin; 13. trans-ferulic acid; 14. hesperidin; 15. isoquercitrin; 16. rutin; 17. quercetin 3-xyloside; 18. kaempferol-3-glucoside; 19. fisetin; 20. quercetin; 21. naringenin.

regression analysis indicated a significant negative correlation between concentration and cell viability against DLD-1, CAPAN-1, and L929. At the concentration of 1 mg/mL, the methanolic extract of *H. perforatum* was maximally effective, resulting in viability of  $33.49 \pm 2.03\%$  and  $48.94 \pm 2.14\%$  for DLD-1 and CAPAN-1, respectively. However, at the concentration of 0.5 mg/mL, we observed an increase to  $71.82 \pm 3.15\%$  against CAPAN-1 cell lines; in contrast, at the concentrations of 0.25 and 0.125 mg/mL no antiproliferative impact was recorded. On the other hand, the antiproliferative activity of the methanolic extract was not significant on L929 cell lines, with cellular activity values ranging from  $109.19 \pm 7.63\%$  to  $419.54 \pm 8.69\%$ . In fact, values above 100% indicate that cells exposed to certain concentrations of the extract displayed higher metabolic activity (MTT reduction) compared to the vehicle control, a phenomenon occasionally observed with plant-derived compounds that can transiently stimulate cell proliferation or mitochondrial activity.<sup>[68]</sup> From these results, the antiproliferative potential of the methanolic extract of *H. perforatum* emerged. This activity may be related to the presence of phenolic compounds and especially flavonoids, which are known as potent antioxidants and antiproliferations.<sup>[69,70]</sup> Previous studies have demonstrated that *H. perforatum* extracts significantly inhibit the proliferation of A549 and HeLa cells at a concentration of 250  $\mu\text{g/mL}$  (Güzey et al., 2011).<sup>[71]</sup> More recently, Yildirim et al.<sup>[72]</sup> approved that hyperforin-rich *H. perforatum* extracts induced apoptosis and reduced viability in breast cancer cell lines, highlighting the effect of phloroglucinols as active cytotoxic constituents. Similarly, Rajnakova et al.<sup>[73]</sup> revealed that methanolic extracts of *H. perforatum* suppressed the growth of human colon cancer cells via ROS-mediated mechanisms, suggesting that the antiproliferative effect is closely related to oxidative stress induction and phenolic enrichment of the extract.

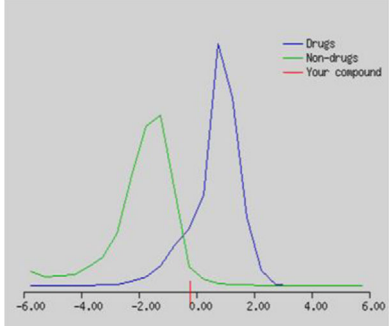
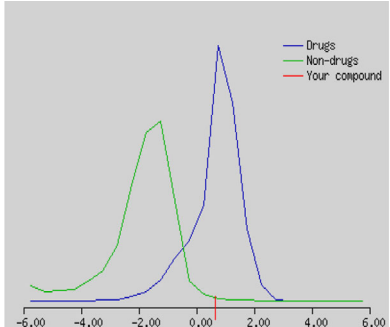
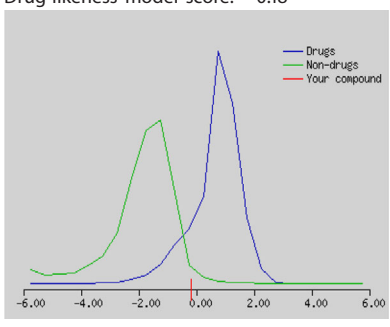
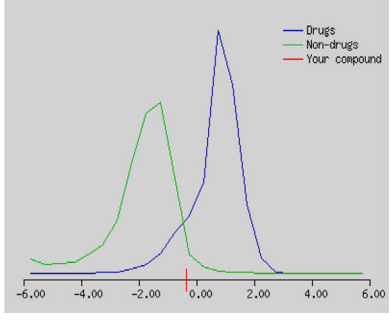
These findings support our results and reinforce the anticancer potential of *H. perforatum* methanolic extract (Figure 7).

### 3.6. Drug-Likeness Properties

SwissADME is a widely used tool in early-stage drug discovery to evaluate the physicochemical and pharmacokinetic properties of bioactive compounds.<sup>[40]</sup> In our study, the database summarized in Table 5 highlights the bioavailability and pharmacokinetic profiles of the identified compounds in the methanolic extract of *H. perforatum*. The molecular weights of the compounds ranged between 154.12 and 448.38, regarding the number of heavy atoms were varied between 11 and 32. However, the topological polar surface area values were mostly above  $70 \text{ \AA}^2$ , except for hydroxybenzaldehyde, vanillic acid, caffeine, and *o*-coumaric acid, indicating moderate membrane permeability. Moreover, all tested compounds had consensus log *P* values  $< 5$ , indicating favorable lipophilicity and confirming their potential as orally active drugs. High gastrointestinal (GI) absorption was predicted for most compounds, which is consistent with the parameters defined by Veber et al.<sup>[74]</sup> regarding the role of molecular flexibility and polar surface area in oral absorption. Only three compounds hydroxybenzaldehyde, *o*-coumaric acid, and trans-ferulic acid were predicted to cross the blood brain barrier (BBB), which is in line with the role of topological polar surface area in central nervous system penetration.<sup>[75]</sup> In terms of drug-likeness, 15 out of 17 compounds satisfied Lipinski's rule of five, and the bioavailability scores ranged from 0.11 to 0.85, suggesting acceptable oral bioavailability. Most compounds exhibited high GI absorption, whereas only hydroxybenzaldehyde, *o*-coumaric acid, and trans-ferulic acid were predicted to cross



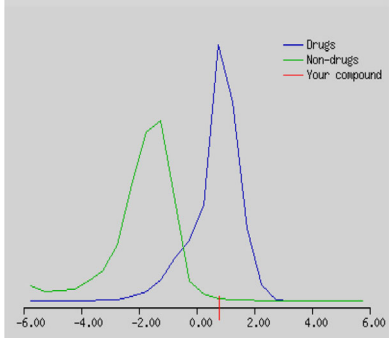
**Table 6.** SMILES, Lipinski's rule of five, and drug-likeness of some compounds predicted using molsoft programme.

No.	Smiles	Molecular properties	Drug-likeness
1	Gallic acid <chem>C1 = C(C = C(C(=C1O)O)O)C(=O)O</chem>	Molecular formula: C <sub>7</sub> H <sub>6</sub> O <sub>5</sub> Number of HBA: 5 Number of HBD: 4 MolLogP: 0.78 MolLogS: -1.10 (in Log(moles/L)) 13,467.71 (in mg/L) MolPSA: 77.22 Å <sup>2</sup> MolVol: 142.94 Å <sup>3</sup> Number of stereo centers: 0 BBB Score: 2.52	Drug-likeness model score: -0.22 
2	Catechin <chem>C1C(OC2 = CC(=CC(=C21)O)O)C3 = CC(=C(C = C3)O)O</chem>	Molecular formula: C <sub>15</sub> H <sub>14</sub> O <sub>6</sub> Number of HBA: 6 Number of HBD: 5 MolLogP: 0.53 MolLogS: -1.45 (in Log(moles/L)) 10,390.50 (in mg/L) MolPSA: 90.45 Å <sup>2</sup> MolVol: 261.13 Å <sup>3</sup> Number of stereo centers: 2 BBB Score: 2.73	Drug-likeness model score: 0.64 
3	Vanillic acid <chem>COC1 = C(C = CC(=C1)C(=O)O)O</chem>	Molecular formula: C <sub>8</sub> H <sub>8</sub> O <sub>4</sub> Number of HBA: 4 Number of HBD: 2 MolLogP: 1.20 MolLogS: -1.94 (in Log(moles/L)) 1920.65 (in mg/L) MolPSA: 52.83 Å <sup>2</sup> MolVol: 152.27 Å <sup>3</sup> Number of stereo centers: 0 BBB Score: 2.86	Drug-likeness model score: -0.18 
4	Caffeic acid <chem>C1 = CC(=C(C = C1C = CC(=O)O)O)O</chem>	Molecular formula: C <sub>9</sub> H <sub>8</sub> O <sub>4</sub> Number of HBA: 4 Number of HBD: 3 MolLogP: 1.27 MolLogS: -1.71 (in Log(moles/L)) 3541.88 (in mg/L) MolPSA: 61.72 Å <sup>2</sup> MolVol: 174.88 Å <sup>3</sup> Number of stereo centers: 0 BBB Score: 2.80	Drug-likeness model score: -0.35 

the BBB. Overall, this database indicate that the majority of the compounds are flexible, moderately polar, soluble, permeable, and small in size, supporting their potential oral bioavailability (Table 5).

### 3.7. Chemical Structure and Bioavailability Radar

The bioavailability radar includes the two-dimensional (2D) image from the JChem webserver and the canonical SMILES

Table 6. (Continued)			
No.	Smiles	Molecular properties	Drug-likeness
5	Caffein CN1C = NC2 = C1C(=O)N(C(=O)N2C)C	Molecular formula: C <sub>8</sub> H <sub>10</sub> N <sub>4</sub> O <sub>2</sub> Number of HBA: 3 Number of HBD: 0 MolLogP: −0.08 MolLogS: −0.75 (in Log(moles/L)) 34,640.54 (in mg/L) MolPSA: 43.79 Å <sup>2</sup> MolVol: 205.73 Å <sup>3</sup> Number of stereo centers: 0 BBB Score: 4.05	Drug-likeness model score: 0.77 

calculated from PubChem that present each molecule per row. The radar defines six important physicochemical properties: lipophilicity, size, polarity, solubility, flexibility and unsaturation. A range of optimal values is illustrated as a pink area and is suitable to be considered drug-like (Figure 8).

### 3.8. Boiled-Egg Model

In SwissADME, the hard-boiled egg is a graphical tool applied to predict the gastrointestinal absorption and brain access of small chemical entities (Figure 9). The white region showing the physicochemical space for a gastrointestinal absorption (highly probable), shows that the following molecules (no. 1, 2, 3, 4, 7, 8, 9, 10, 12, 19, 20, and 21), are predicted to have a high GI absorption when taken orally. On the other side, the yellow region (yolk), representing the physicochemical space for a highly probable BBB permeation, refers to molecules that have the ability to penetrate the BBB; this is what has been demonstrated for molecules no. 6, 11, and 13, which therefore can have a significant effect on the central nervous system. Thus, from the graph we get a global analysis of passive absorption (in/out of the egg white) and passive access to the brain (in/out of the yolk). The hard-boiled egg is color-coded: blue dots for P-gp substrates (PGP+) and red dots for non-P-gp substrates (PGP−); molecules falling outside the egg are considered less absorbent and less penetrating the BBB (no. 5, 17, and 18).

After taking the physicochemical and pharmacokinetic analyses, pKCSM was used by introducing the SMILES code of each molecule (Table 6). The results of this in silico analysis were presented in Table 6. In fact, pKCSM database provides valuable insights into the safety and toxicity profiles and the tolerated dose for humans and other properties of the identified compounds.<sup>[76]</sup> Compounds like Pyrocatechol and Theobromine should be handled with caution due to their toxicity and mutagenic potential, respectively. On the other hand, compounds like Caffeic Acid and Ferulic Acid appear to be safer for human use based on their higher tolerated doses and lower toxicity profiles.

### 3.9. In Silico Toxicological Predictions of Selected Phenolic Compounds

The in silico toxicity predictions indicated that all examined compounds were non-mutagenic according to the AMES test, suggesting the absence of genotoxic risk. Maximum tolerated dose values diversified between compounds, with syringic acid, caffeic acid, and *o*-coumaric acid exhibiting the highest tolerance, whereas naringenin and chlorogenic acid presented lower tolerance values (Table 7). Acute oral toxicity (rat LD<sub>50</sub>) predictions demonstrated that most compounds fell within a relatively safe range (2.2–2.5 mol/kg), with caffeine exhibiting the highest LD<sub>50</sub>, and naringenin appearing as the most acutely toxic compound. Concerning hepatotoxicity, caffeine was the only compound predicted to exert adverse effects on the liver, whereas all other metabolites displayed no hepatotoxic potential. None of the compounds were predicted to act as skin sensitizers, highlighting a favorable dermatological safety profile. Overall, these results emphasize that the majority of the investigated secondary metabolites from *H. perforatum* and are predicted to be safe. However, excepting caffeine, which requires careful consideration due to its hepatotoxic potential.

## 4. Conclusion

The aerial parts of *H. perforatum* were found to be a potent source of bioactive substances with antioxidant and antiproliferative properties. The online servers “SwissADME” provided us with a rapid approach for the identification of active compounds whereas the web tool “pKCSM” allowed us to determine the toxicity of the identified molecules, which is a critical parameter in drug design. The results obtained in this study provide a scientific basis for improving the use of natural matrices widely used in traditional medicine. In conclusion, *H. perforatum* was found to possess promising therapeutic properties and could be a good candidate as an effective adaptogenic herbal remedy.

**Table 7.** Predicted toxicity profiles of identified compounds in the methanolic extract of *H. perforatum* using pkCSM.

No.	Compound	AMES toxicity	Max. tolerated dose (human) (log mg/kg/day)	Oral rat acute toxicity (LD <sub>50</sub> ) (mol/kg)	Hepatotox	Skin sens.
1	Gallic acid	No	0.7	2.218	No	No
2	Protocatechuic acid	No	0.814	2.423	No	No
3	Epigallocatechin	No	0.506	2.492	No	No
4	Catechin	No	0.438	2.428	No	No
5	Chlorogenic acid	No	−0.134	1.973	No	No
6	Hydroxybenzaldehyde	No	1.135	1.893	No	No
7	Vanillic acid	No	0.719	2.454	No	No
8	Caffeic acid	No	1.145	2.383	No	No
9	Syringic acid	No	1.374	2.157	No	No
10	Caffein	No	0.001	2.802	Yes	No
11	<i>o</i> -Coumaric acid	No	1.132	2.192	No	No
12	Polydatin	No	0.569	2.516	No	No
13	Trans-ferulic acid	No	1.082	2.282	No	No
14	Hesperidin	No	0.525	2.506	No	No
15	Isoquercitrin	No	0.569	2.541	No	No
16	Rutin	No	0.452	2.491	No	No
17	Quercetin 3-xyloside	No	0.576	2.543	No	No
18	Kaempferol-3-glucoside	No	0.582	2.546	No	No
19	Fisetin	No	0.579	2.465	No	No
20	Quercetin	No	0.499	2.471	No	No
21	Naringenin	No	−0.176	1.791	No	No
22	Kaempferol	No	0.531	2.449	No	No

AMES: mutagenicity; hepatotox: hepatotoxicity; skin sens: skin sensitization.

## Author Contributions

**L.R.:** Investigation; writing—original draft; software; formal analysis. **H.B.:** supervision; writing—review and editing. **C.H.S.:** Conceptualization; validation; supervision. **L.D.:** Investigation. **L.R.:** Writing—original draft. **A.M.M.:** Formal analysis. **P.R.V.:** Project administration; supervision; writing—review and editing. **I.D.:** Project administration. **S.G.:** Writing—review and editing; supervision. **F.B.:** Investigation; formal analysis. All authors have read and agreed to the published version of the manuscript.

## Acknowledgments

The authors have nothing to report.

## Conflict of Interests

The authors declare no conflict of interest.

## Data Availability Statement

The data that support the findings of this study are available from the corresponding author upon reasonable request.

**Keywords:** Biological activities · *Hypericum perforatum* · In silico ADME · LC-ESI-MS/MS · Phenolic compounds

- [1] G. I. Caldeira, L. P. Gouveia, R. Serrano, O. D. Silva, *Plants* **2022**, *11*, 2509, <https://doi.org/10.3390/plants11192509>.
- [2] N. K. Robson, *Systematics and Biodiversity* **2006**, *4*, 19–98.
- [3] E. E. Özkan, A. Mat, *J. Pharmacogn. Phytother.* **2013**, *5*, 38–46.
- [4] L. Roumaissa, C. H. Saida, L. Derbak, N. Raniya, D. Ibrahim, B. Hamdi, *Brazilian J. Health Rev.* **2025**, *8*, e76834, <https://doi.org/10.34119/bjhrv8n1-195>.
- [5] J. Drożdżał, O. Barańska, M. Chańko, A. Krzaczkowski, E. Niedzielska, M. Rędaszka, J. Szuba, Z. Szular, T. Wojczulis, K. Ziemek, *Quality in Sport* **2025**, *42*, 60806–60806.
- [6] M. Al-Akoun, E. Maunsell, R. Verreault, L. Provencher, H. Otis, S. Dodin, *Menopause* **2009**, *16*, 307–314.
- [7] E. Bombardelli, P. Morazzoni, *Fitoterapia* **1995**, *66*, 43–68.
- [8] A. Alghamdi, *Bull. Pharmaceut. Sci. Assiut Univ.* **2025**, *48*, 277–294.
- [9] M. V. Suryawanshi, P. P. Gujarathi, T. Mulla, I. Bagban, *Naunyn-Schmiedeberg's Archives of Pharmacol.* **2024**, *397*, 3803–3818, <https://doi.org/10.1007/s00210-023-02915-6>.
- [10] R. Bagheri, S. Bohloul, S. Maleki Dizaj, S. Shahi, M. Y. Memar, S. Salatin, *Clinics and Practice* **2022**, *12*, 1009–1019, <https://doi.org/10.3390/clinpract12060104>.
- [11] R. Moeinzadeh, M. Hekmati, N. Azizi, M. Qomi, D. Esmaeili, *Chem. Rev. Lett.* **2024**, *7*, 185–200.
- [12] M. Ç. Ayvaz, G. Aydoğdu, Z. Koloren, O. Kolören, P. Karanis, *Turkish J. Weed Sci.* **2023**, *26*, 49–57.
- [13] D. Dincel, Y. Dari, Ç. K. Hançer, N. B. Onal, M. Kartal, G. Topçu, *Turkish J. Analyt. Chem.* **2025**, *7*, 1–8, <https://doi.org/10.51435/turkjac.1565559>.

- [14] O. B. Akkaya, İ. S. Çelik, E. Ertaş, N. Çömlekcioglu, A. Aygan, *Int. J. Chem. Technol.* **2024**, *8*, 73–82, <https://doi.org/10.32571/ijct.1445857>.
- [15] L. H. Bajrai, S. A. El-Kafrawy, A. M. Hassan, A. M. Tolah, R. S. Alnahas, S. S. Sohrab, M. Rehan, E. I. Azhar, *Sci. Rep.* **2022**, *12*, 21723, <https://doi.org/10.1038/s41598-022-26157-3>.
- [16] A. Brankiewicz, S. Trzos, M. Mrozek, M. Opydo, E. Szostak, M. Dziurka, M. Tuleja, A. Loboda, E. Pocheć, *Molecules* **2023**, *28*, 1509, <https://doi.org/10.3390/molecules28031509>.
- [17] I. Raczkiwicz, C. Rivière, P. Bouquet, L. Desmarests, A. Tarricone, C. Camuzet, N. François, G. Lefèvre, F. S. Angulo, C. Robil, F. Trottein, S. Sahpaz, J. Dubuisson, S. Belouzard, A. Goffard, K. Séron, *Front. Microbiol.* **2024**, *15*, 1443183, <https://doi.org/10.3389/fmicb.2024.1443183>.
- [18] L. R. Haake, A. El Menuawy, H. Rennau, F. Marthe, U. Hähnel, F. Bock, G. Hildebrandt, K. Manda, *Int. J. Mol. Sci.* **2025**, *26*, 622, <https://doi.org/10.3390/ijms26020622>.
- [19] P. Agostinis, A. Vantieghe, W. Merlevede, P. A. de Witte, *Int. J. Biochem. Cell Biol.* **2002**, *34*, 221–241.
- [20] J. Piette, C. Volanti, A. Vantieghe, J. Y. Matroule, Y. Habraken, P. Agostinis, *Biochem. Pharmacol.* **2003**, *66*, 1651–1659, [https://doi.org/10.1016/S0006-2952\(03\)00539-2](https://doi.org/10.1016/S0006-2952(03)00539-2).
- [21] N. S. Radulović, M. S. Genčić, N. M. Stojanović, P. J. Randjelović, N. Baldovini, V. Kurteva, *Food Chem. Toxicol.* **2018**, *118*, 505–513, <https://doi.org/10.1016/j.fct.2018.05.009>.
- [22] M. Saffariha, A. Jahani, R. Jahani, S. Latif, *Plant Methods* **2021**, *17*, 10, <https://doi.org/10.1186/s13007-021-00710-z>.
- [23] W. D'Alger, M. de Paris, Guide Illustré de la Flore Algérienne. Délégation Générale aux Relations Internationales, Ville de Paris, **2012**.
- [24] P. Quezel, S. Santa, New flora of Algeria and southern desert regions, **1962**.
- [25] K. Makarova, J. J. Sajkowska-Kozielewicz, K. Zawada, E. Olchowik-Grabarek, M. A. Ciach, K. Gogolewski, N. Dobros, P. Ciechowicz, H. Freichels, A. Gambin, *Sci. Rep.* **2021**, *11*, 3989.
- [26] B. Le Dare, T. Gicquel, *J. Pharma. Pharmaceut. Sci.* **2019**, *22*, 525–535, <https://doi.org/10.18433/jpps30572>.
- [27] L. Derbak, H. Bendif, R. Ayad, K. Rebbas, I. Demirtas, I. Yildiz, F. Boufahja, S. Garzoli, *Food Analyt. Meth.* **2025**, 1–16.
- [28] C. M. Griffith, Thai, C. K. Larive, *Sci. Total Environ.* **2019**, *681*, 435–443, <https://doi.org/10.1016/j.scitotenv.2019.04.312>.
- [29] M. Köktürk, M. N. Atalar, A. Odunkiran, M. Bulut, D. Alwazeer, *Environ. Sci. Pollut. Res.* **2022**, *29*, 19642–56.
- [30] M. A. Yilmaz, *Ind. Crops Prod.* **2020**, *149*, 112347, <https://doi.org/10.1016/j.indcrop.2020.112347>.
- [31] V. L. Singleton, R. Orthofer, R. M. Lamuela-Raventós, *Methods in Enzymol.* **1999**, *299*, 152–178.
- [32] P. Prieto, M. Pineda, M. Aguilar, *Anal. Biochem.* **1999**, *269*, 337–341, <https://doi.org/10.1006/abio.1999.4019>.
- [33] R. M. J. N. Srinivasan, M. J. N. Chandrasekar, M. J. Nanjan, B. Suresh, *J. Ethnopharmacol.* **2007**, *113*, 284–291, <https://doi.org/10.1016/j.jep.2007.06.006>.
- [34] R. Re, N. Pellegrini, A. Proteggente, A. Pannala, M. Yang, C. Rice-Evans, *Free Radical Biol. Med.* **1999**, *26*, 1231–1237, [https://doi.org/10.1016/S0891-5849\(98\)00315-3](https://doi.org/10.1016/S0891-5849(98)00315-3).
- [35] N. Kartal, M. Sokmen, B. Tepe, D. Daferera, M. Polissiou, A. Sokmen, *Food Chemistry* **2007**, *100*, 584–589.
- [36] M. Oyaizu, *Japanese J. Nutr. Diet.* **1986**, *44*, 307–315, <https://doi.org/10.5264/eiyogakuzashi.44.307>.
- [37] R. Apak, K. Güçlü, B. Demirata, M. Özyürek, S. E. Çelik, B. Bektaşoğlu, B. Bektaşoğlu, K. I. Berker, D. Özyurt, *Molecules* **2007**, *12*, 1496–1547, <https://doi.org/10.3390/12071496>.
- [38] R. L. Prior, H. A. Hoang, L. Gu, X. Wu, M. Bacchiocca, L. Howard, M. Hampsch-Woodill, D. Huang, B. Ou, R. Jacob, *J. Agric. Food Chem.* **2003**, *51*, 3273–3279, <https://doi.org/10.1021/jf0262256>.
- [39] S. Ameur, M. Touni, H. Bendif, L. Derbak, I. Yildiz, K. Rebbas, I. Demirtas, G. Flamini, M. Bruno, S. Garzoli, *J. Food Compos. Anal.* **2024**, *136*, 106747, <https://doi.org/10.1016/j.jfca.2024.106747>.
- [40] A. Daina, O. Michielin, V. Zoete, *Sci. Rep.* **2017**, *7*, 42717, <https://doi.org/10.1038/srep42717>.
- [41] D. E. V. Pires, T. L. Blundell, D. B. Ascher, *J. Med. Chem.* **2015**, *58*, 4066–4072, <https://doi.org/10.1021/acs.jmedchem.5b00104>.
- [42] A. N. Tamfu, S. Kucukaydin, M. M. Quradha, O. Ceylan, A. Ugur, M. E. Duru, *Chem. Afr.* **2022**, *5*, 237–249, <https://doi.org/10.1007/s42250-022-00315-6>.
- [43] F. Maggi, G. Ferretti, N. Pocceschi, L. Menghini, M. Ricciutelli, *Fitoterapia* **2004**, *75*, 702–711.
- [44] S. M. A. Zobayed, F. Afreen, E. Goto, T. Kozai, *Annals of Botany* **2006**, *98*, 793–804, <https://doi.org/10.1093/aob/mcl169>.
- [45] A. Nahrstedt, V. Butterweck, *Pharmacopsychiatry* **1997**, *30*, 129–134, <https://doi.org/10.1055/s-2007-979533>.
- [46] H. Wagner, S. Bladt, *J. Geriatr. Psychiatr. Neurol.* **1994**, *7*, 65–68, <https://doi.org/10.1177/089198879400700118>.
- [47] A. Aslam, S. Zhao, X. Lu, N. He, H. Zhu, A. U. Malik, M. Azam, W. Liu, *Biomolecules* **2021**, *11*, 628, <https://doi.org/10.3390/biom11050628>.
- [48] G. Piatti, C. Ciaramelli, S. Vitalini, *Plants* **2023**, *12*, 1765.
- [49] I. E. Orhan, *Turkish J. Pharmaceut. Sci.* **2015**, *12*.
- [50] G. Zdunic, D. Godjevac, K. Savikin, S. Petrovic, *Natur. Prod. Commun.* **2017**, *12*, <https://doi.org/10.1177/1934578X1701201140>.
- [51] J. Zvezdanović, *Chem. Pap.* **2022**, *76*, 1329–1347, <https://doi.org/10.1007/s11696-021-01940-0>.
- [52] X. Moreira, J. Durán, A. Rodríguez, A. Cao, M. Correia, J. Seródio, S. Rodríguez-Echeverría, *Plant Biol.* **2025**, *27*, 417–425, <https://doi.org/10.1111/plb.13776>.
- [53] W. Sun, M. H. Shahrajabian, *Molecules* **2023**, *28*, 1845, <https://doi.org/10.3390/molecules28041845>.
- [54] E. Ersoy, E. E. Ozkan, M. Boga, & A. Mat, *South Afr. J. Botany* **2020**, *130*, 141–147.
- [55] S. Marah, İ. Demirtas, T. Ozen, *Int. J. Chem. Technol.* **2022**, *6*, 164–169, <https://doi.org/10.32571/ijct.1187768>.
- [56] D. S. Stef, G. Iosif, T. Ioan-Trasca, L. Stef, C. Pop, M. Harmanescu, R. Biron, E. Pet, Evaluation of 33 medicinal plant extracts for the antioxidant capacity and total phenols, **2010**.
- [57] E. Ersoy, E. E. Ozkan, M. Boga, A. Mat, *South Afr. J. Botany* **2020**, *130*, 141–147, <https://doi.org/10.1016/j.sajb.2019.12.017>.
- [58] E. E. Özkan, A. Mat, *J. Pharmacogn. Phytother.* **2013**, *5*, 38–46.
- [59] A. Antony, M. Farid, *Appl. Sci.* **2022**, *12*, 2107, <https://doi.org/10.3390/app12042107>.
- [60] S. A. A. Jafri, Z. M. Khalid, M. Z. Khan, N. Jogezi, *Open Chem.* **2022**, *20*, 1337–1356, <https://doi.org/10.1515/chem-2022-0242>.
- [61] M. Cengiz, O. Yildiz, H. Çelik, *J. Food Biochem.* **2020**, *44*, e13193.
- [62] E. Kakouri, P. Trigas, D. Daferera, E. Skotti, P. A. Tarantilis, C. Kanakis, *Antioxidants* **2023**, *12*, 899, <https://doi.org/10.3390/antiox12040899>.
- [63] Y. Tumbarski, I. Ivanov, M. Todorova, A. Gerasimova, I. Dincheva, L. Makedonski, K. Nikolova, *Appl. Sci.* **2024**, *14*, 11754.
- [64] E. Błońska-Sikora, K. Gach, J. Cielecka-Piontek, S. Ślusarczyk, *Antioxidants* **2025**, *14*, 215.
- [65] A. Doğan, A. Kaya, N. Öztürk, *Plants* **2024**, *13*, 621.
- [66] B. Kurt, L. Aksoy, A. Özkan, *J. Mol. Struct.* **2025**, *1364*, 135276.
- [67] M. Katsarova, S. Dimitrova, L. Lukanov, F. Sadakov, P. Denev, E. Plotnikov, I. Kostadinova, *Bulg. Chem. Commun.* **2017**, *49*, 93–98.
- [68] M. Ghasemi, T. Turnbull, S. Sebastian, I. Kempson, *Int. J. Mol. Sci.* **2021**, *22*, 12827, <https://doi.org/10.3390/ijms222312827>.
- [69] R. Chahna, H. Bendif, A. Bouzana, L. Derbak, I. Haouame, D. Çam, M. Öztürk, K. Rebbas, M. A. Ali, C. Bensouici, F. Boufahja, S. Garzoli, *Food Analyt. Meth.* **2025**, 1–19.
- [70] L. Derbak, H. Bendif, R. Ayad, C. Bensouici, İ. Yildiz, I. Demirtas, K. Rebbas, G. Plavan, N. B. Hamadi, A. M. Abu-Elsaoud, M. M. Alomran, S. Özdemir, F. Boufahja, *Open Chem.* **2024**, *22*, 20240040, <https://doi.org/10.1515/chem-2024-0040>.
- [71] G. Güzey, S. Ibadova, Y. Öztürk, N. Öztürk, F. Maggi, G. Sagratini, S. Vittori, *Medicinal and Aromatic Plant Science and Biotechnology* **2011**, *5*, 91–99.
- [72] A. B. Yildirim, A. U. Turker, A. C. Goren, *J. Ethnopharmacol.* **2022**, *285*, 114867.
- [73] A. Rajnakova, R. Simeonova, D. Zheleva, S. Dimitrova, *Biomed. Pharmacother.* **2023**, *163*, 114782.



- [74] D. F. Veber, S. R. Johnson, H. Y. Cheng, B. R. Smith, K. W. Ward, K. D. Kopple, *J. Med. Chem.* **2002**, *45*, 2615–2623, <https://doi.org/10.1021/jm020017n>.
- [75] P. Ertl, B. Rohde, P. Selzer, *J. Med. Chem.* **2000**, *43*, 3714–3717, <https://doi.org/10.1021/jm000942e>.
- [76] N. A. Durán-Iturbide, B. I. Díaz-Eufracio, J. L. Medina-Franco, *ACS Omega* **2020**, *5*, 16076–16084, <https://doi.org/10.1021/acsomega.0c01581>.

---

Manuscript received: June 24, 2025